Current Research in Food Science 9 (2024) 100888

Contents lists available at ScienceDirect

Current Research in Food Science

journal homepage: www.sciencedirect.com/journal/current-research-in-food-science

Targeting protein aggregation using a cocoa-bean shell extract to reduce α-synuclein toxicity in models of Parkinson's disease

Farida Tripodi [a,b], Alessia Lambiase [a,b], Hind Moukham [a], Giorgia Spandri [a], Maura Brioschi [a], Ermelinda Falletta [c], Annalisa D'Urzo [a], Marina Vai [a], Francesco Abbiati [a], Stefania Pagliari [a], Andrea Salvo [d], Mattia Spano [d], Luca Campone [a,b], Massimo Labra [a,b], Paola Coccetti [a,b,*]

[a] Department of Biotechnology and Biosciences, University of Milano-Bicocca, Milano, Italy
[b] National Biodiversity Future Center (NBFC), Palermo, Italy
[c] Department of Chemistry, University of Milano, Milano, Italy
[d] Department of Chemistry and Drug Technology, University of Roma La Sapienza, Roma, Italy

ARTICLE INFO

Handling Editor: Dr. Yeonhwa Park

Keywords:
Saccharomyces cerevisiae
Human α-synuclein
Parkinson's disease (PD)
Cocoa
Food waste valorization

ABSTRACT

Neurodegenerative diseases are among the major challenges in modern medicine, due to the progressive aging of the world population. Among these, Parkinson's disease (PD) affects 10 million people worldwide and is associated with the aggregation of the presynaptic protein α-synuclein (α-syn). Here we use two different PD models, yeast cells and neuroblastoma cells overexpressing α-syn, to investigate the protective effect of an extract from the cocoa shell, which is a by-product of the roasting process of cocoa beans. The LC-ESI-qTOF-MS and NMR analyses allow the identification of amino acids (including the essential ones), organic acids, lactate and glycerol, confirming also the presence of the two methylxanthines, namely caffeine and theobromine. The present study demonstrates that the supplementation with the cocoa bean shell extract (CBSE) strongly improves the longevity of yeast cells expressing α-syn, reducing the level of reactive oxygen species, activating autophagy and reducing the intracellular protein aggresomes. These anti-aggregation properties are confirmed also in neuroblastoma cells, where CBSE treatment leads to activation of AMPK kinase and to a significant reduction of toxic α-syn oligomers. Results obtained by surface plasmon resonance (SPR) assay highlights that CBSE binds α-syn protein in a concentration-dependent manner, supporting its inhibitory role on the amyloid aggregation of α-syn. These findings suggest that the supplementation with CBSE in the form of nutraceuticals may represent a promising way to prevent neurodegenerative diseases associated with α-syn aggregation.

1. Introduction

The food industry produces a high amount of waste during food processing and production. Under a circular economy perspective, the valorization of these by-products and waste is convenient not only from an economic and environmental point of view, but also because they are rich in active compounds with potentially useful bioactivities (Oreopoulou and Russ, 2007; Panak Balentić et al., 2018).

Cocoa beans (*Theobroma cacao* L.) are widely used in food production, but also for pharmaceutical and cosmetic purposes (Mazzutti et al., 2018). One of the main by-product of cocoa processing is the cocoa bean shell, which is produced in large quantities during the roasting process (Panak Balentić et al., 2018; Okiyama et al., 2017). It has been estimated that global cocoa bean production in the 2015/2016 harvest reached approximately 3972 thousand tons, with the shell making up to 20% of the bean (Okiyama et al., 2018; Soares and Oliveira, 2022). This represents roughly 600 thousand tons, most of which are discarded as waste and remain under-utilised, with limited applications as boiler fuel, animal feed, or fertilizer (Okiyama et al., 2018). However, in recent years, cocoa shells have gained attention as a rich source of phenolic compounds, including caffeine and theobromine (Okiyama et al., 2018; Arlorio et al., 2005; Pagliari et al., 2022; Visioli et al., 2012; Gil-Ramírez et al., 2024). These two compounds, belonging to the methylxanthine class, are well-known for their antioxidant and anti-inflammatory properties (Rebollo-Hernanz et al., 2019, 2022; Cadoná et al., 2022), which contribute to mitigating oxidative stress, a key factor in neurodegenerative diseases. While the spotlight is often on cocoa bean, recent studies suggest that cocoa shells, given their abundant availability and

* Corresponding author. Department of Biotechnology and Biosciences, University of Milano-Bicocca, Milano, Italy.
E-mail address: paola.coccetti@unimib.it (P. Coccetti).

https://doi.org/10.1016/j.crfs.2024.100888
Received 17 August 2024; Received in revised form 9 October 2024; Accepted 16 October 2024
Available online 24 October 2024

cost-effectiveness, can offer a significant potential as a sustainable resource for developing therapeutic agents (Rojo-Poveda et al., 2020; Cinar et al., 2021; Sánchez et al., 2023). Besides, new insights into the toxicological safety of two cocoa shell matrices has been also provided, opening opportunities for their use as functional food and nutraceutical products (Gil-Ramírez et al., 2024). Recently, a new environmentally friendly and automated pressurised liquid extraction method has been developed and optimised to selectively recover theobromine and caffeine from cocoa shell by-products (Pagliari et al., 2022).

Parkinson's disease (PD), characterised by aberrant aggregates of the presynaptic protein α-synuclein (α-syn), is the second most common neurodegenerative disease (Poewe et al., 2017; Calabresi et al., 2023; Fields et al., 2019). Many *in vitro* and *in vivo* models mimicking α-syn pathology have been used over the years (Delenclos et al., 2019); among them, *Saccharomyces cerevisiae* has been extensively employed as a model of synucleinopathies (Fruhmann et al., 2017; Sampaio-Marques et al., 2018, 2019; Tenreiro et al., 2017). This unicellular eukaryote is a valuable tool in research due to its small size, short generation time, non-pathogenic nature, and ease of genetic manipulation (Longo et al., 2012). The deep conservation of cellular mechanisms, such as DNA replication, cell division, and protein folding, from yeast to pluricellular eukaryotes, underscores its relevance for human disease studies. The most commonly used yeast model for Parkinson's disease research involves the heterologous expression of human α-syn, which induces toxicity associated with aggregate formation, leading to vesicular trafficking impairment, increased oxidative stress and mitochondrial dysfunction, reduced lifespan, disturbed calcium signaling and altered autophagy (Sampaio-Marques et al., 2018, 2019; Tenreiro et al., 2016; Outeiro and Lindquist, 2003; Büttner et al., 2008). As in more complex systems, the autophagic pathway is the major responsible for the clearance of oligomers and toxic aggregates, which cannot be degraded by the proteasome (Popova et al., 2015).

Although *S. cerevisiae* provides an excellent platform for preliminary studies, pluricellular eukaryotic models such as *Caenorhabditis elegans* (da Silva et al., 2024; Hughes et al., 2022), *Drosophila melanogaster* (Sanz et al., 2017; Avallone et al., 2024) and mice (Dovonou et al., 2023) are also extensively employed. Interestingly, a SH-SY5Y cell line overexpressing α-syn through a doxycycline-inducible promoter, is a valuable model for studying the molecular mechanisms underlying neuronal degeneration (Vasquez et al., 2018). This eukaryotic system provides a robust platform for the *in vitro* screening of neuroprotective compounds to evaluate potential pharmaceutical compounds.

Here we show that an extract from cocoa bean shells increases lifespan and reduces reactive oxygen species (ROS) levels in a yeast model of synucleinopathy. Its anti-aging properties are associated with a stimulation of autophagy during the first two days of the stationary phase and a strong anti-aggregation feature both *in vivo* and *in vitro*. Consistently, our data also highlight a significant reduction of toxic α-syn oligomers in neuroblastoma cells expressing α-syn, supporting the potential use of cocoa bean shell extract as a preventive agent against aggregation and its pathogenic effects.

2. Materials and methods

2.1. Chemical reagents

All chemicals were purchased from Merck unless otherwise stated. MS-grade solvents used for UPLC analysis, acetonitrile, water, and formic acid were provided by Romil. Reagents for SPR experiments were purchased from Cytiva. Cell culture media and supplements were provided by Euroclone, Biolog plates and reagents were provided by Rigel Process and Lab.

2.2. Cocoa bean shell extract (CBSE) preparation

Cocoa bean shell (Trinitario variety) was kindly provided by a cocoa processor after being roasted at 225 °C for approximately 20 min. The cocoa bean shell extract (CBSE) was obtained by Pressurised Liquid Extraction (PLE) using Dionex ASE350 (Dionex Sunnyvale, CA) as previously reported (Pagliari et al., 2022). Briefly, 1 g of dry matrix, previously blended and sieved (300–600 μm) to obtain homogeneous samples, was extracted in 5 mL stainless steel cells using 15% EtOH solution, 90 °C temperature, 5 cycles and a static time of 6 min at a pressure of 100 bar. After the extraction the ethanol was removed using a rotary evaporator (G3, heiVAP core, Heidolph Germany) with the bath temperature set at 40 °C and the extract was freeze-dried (ALPHA 1–2 LSC BASIC, Christ Germany) with a yield of 20.68 ± 1.25 % of dry matrix.

2.3. Chemical characterization and quantitative analysis of caffeine and theobromine

The CBSE was analysed by Synapt G2-Si QToF instrument (equipped with a ZsprayTM ESI-probe) (Waters) coupled with an Acquity UPLC I-Class chromatography system (Waters). The UPLC analyses were carried out by a ACQUITY UPLC HSS T3 column (100 × 2.1 mm, 1.8 μm, Waters) fitted with a VanGuard cartridge (Waters) maintained at a fixed temperature of 35 °C. The products were separated using a linear gradient elution program, which consisted of water (A) and acetonitrile (B) (both with 0.1% formic acid) varying from 5 to 95% B (0–20 min). A flow rate of 0. 4 mL/min and an injection volume of 4 μL were adopted. The PDA acquisition wavelength range was 190–400 nm. For mass spectrometry analyses, both negative and positive ionization modes were applied. The ESI-modes were acquired in the range of 50–1200 m/z with a fixed source temperature of 120 °C and a desolvation temperature of 150 °C. A desolvation gas flow of 600 L/h was employed. The capillary voltage was 3 kV (positive ionization mode) and −2 kV (negative ionization mode). The instrument was controlled by a MassLynxTM v4.2 software (Waters). All MS acquisitions were performed the same day, with blank control between injections.

For quantitative analysis, the UPLC system was coupled with a UV detector acquiring data 283 nm. An external standard calibration method was used to quantify theobromine and caffeine in the extract. Standard solutions of theobromine and caffeine, each at a concentration of 1 mg/mL, were properly diluted with H_2O to create six-level calibration curves ranging from 1 to 200 μg/mL. The linearity of each calibration curve was verified using analysis of variance (ANOVA), and the linear model was found appropriate for the concentrations used and each level was acquired in triplicate. The instrument was controlled by a MassLynxTM v4.2 software (Waters). All MS acquisitions were performed the same day, with blank control between injections.

In addition, to detect analytes not visible with mass spectrometry, an NMR analysis was also conducted. Extract aliquots (4.3–4.7 mg) were resuspended in 1 mL deuterated water, containing 50 mM phosphate buffer pH7.4 and 0.4 mM TSP (internal standard). 700 μL of this solution were transferred to NMR tubes and analysed. NMR analyses were performed with a JEOL JNM-ECZ 600R spectrometer (resonance 1H 600.17 MHz) equipped with a 5 mm FG/RO DIGITAL AUTOTUNE probe. Monodimensional experiments were carried out in the following conditions: 128 scans, 4 dummy scans, presaturation of the residual water signal, impulse at 90 °C of 8.3 μs, 64K data points, time of acquisition 7.7 s. For metabolite identification, literature data referred to NMR studies on cocoa samples (Caligiani et al., 2010, 2014) were used. To quantify the identified metabolites in the aqueous solution, the integrals of the selected 1H resonances were measured with respect to TSP as previously described (Spano et al., 2024). Three replicates were made, and the results were expressed as μg/mg of extract ± SD.

2.4. Proteomic characterization

Proteins present in the CBSE were concentrated and separated from small molecules using molecular cut-off filtration (Amicon 10000 Da

MWCO, Merck) with two washes with water. After protein precipitation with 80% Acetonitrile, pellets were resuspended in 25 mmol/L NH_4HCO_3 containing 0.1% RapiGest (Waters Corporation) and sonicated by immersion for 10 s before digestion, as previously described (Brioschi et al., 2013). After 15 min of incubation at 80 °C, proteins were reduced with 5 mmol/L DTT at 60 °C for 15 min, and carbamidomethylated with 10 mmol/L iodoacetamide for 30 min at room temperature in darkness. Digestion was performed with sequencing-grade trypsin (Promega) (1 μg every 25 μg of proteins) overnight at 37 °C. After digestion, 2% TFA was added to hydrolyze RapiGest and inactivate trypsin.

Tryptic peptides were used for label-free mass spectrometry analysis, LC-MS^E, which was performed on a hybrid quadrupole time-of-flight mass spectrometer (Xevo G2-XS, Waters Corporation), coupled with a UPLC H-class system and equipped with an ESI source (Waters Corporation). Samples were injected into an analytical column ACQUITY Premier HSS T3 C18, 100 Å, 1.8 μm, 2.1 mm × 150 mm equipped with a vanguard FIT cartridge (Waters Corporation), for elution at a flow rate of 200 μl/min for 3 min at 2% mobile phase B before increasing the organic solvent B concentration from 2 to 50% over 90 min, using 0.1% v/v formic acid in water as reversed phase solvent A, and 0.1% v/v formic acid in acetonitrile as reversed phase solvent B. All of the analyses were performed in duplicate and analysed by LC-MS^E as previously detailed (Brioschi et al., 2014). In particular, in the low-energy MS mode, the data were collected with Masslynx software at a constant collision energy of 6 eV, while in the high-energy mode, fragmentation was achieved by applying a ramp from 15 to 35 eV. Scan time of 0.1 s, capillary voltage of 1 kV, cone voltage of 40 V, source temperature 120 °C, desolvation temperature of 600 °C with desolvation gas at 800 L/h were applied to acquire spectra in the range 50–1990 m/z. The time-of-flight analyzer was externally calibrated using Sodium formate from m/z 50 to 1990, and data were post-acquisition lock mass corrected using the monoisotopic mass of the doubly charged precursor of [Glu1]-fibrinopeptide B (m/z 785.8426) delivered to the mass spectrometer at 100 fmol/μL. The reference sprayer was sampled every 30 s. The radio frequency (RF) applied to the quadrupole mass analyzer was adjusted in such a way that ions from m/z 300 to 2000 were efficiently transmitted, thus ensuring that any ion with a mass of less than m/z 300 only arose from dissociations in the collision cell. Peak detection and protein identification were performed with PLGS software (v 3.0.3) using a Uniprot *Theobroma cocoa* sequence database (v2024_04, 40947 unreviewed entries, 16 reviewed entries) and NCBI database (167551 entries). The following search criteria were used for protein identification: the default search parameters included the "automatic" setting for mass accuracy (approximately 10 ppm for precursor ions and 25 ppm for product ions); a minimum of one peptide match per protein, a minimum of two consecutive product ion matches per peptide, and a minimum of five total product ion matches per protein; up to one missed cleavage site allowed; carbamidomethyl-cysteine as fixed modification; and methionine oxidation as variable modification.

Table 1
Yeast strains used in this study.

Yeast strain	Genotype	Source
wt [empty]	*BY4742 MATα his3Δ1 leu2Δ0 lys2Δ0 ura3Δ0 [pYX242]*	Tripodi et al. (2020)
wt [αSyn]	*BY4742 MATα his3Δ1 leu2Δ0 lys2Δ0 ura3Δ0 [pYX242-SNCA]*	Tripodi et al. (2020)
wt [αSyn] [ATG8-GFP]	*BY4742 MATα his3Δ1 leu2Δ0 lys2Δ0 ura3Δ0 [pYX242-SNCA][pCu-ATG8-GFP]*	Tripodi et al. (2022)
atg8Δ [αSyn]	*BY4742 MATα his3Δ1 leu2Δ0 lys2Δ0 ura3Δ0 atg8Δ::KanMX [pYX242-SNCA]*	This study

2.5. Yeast strains, growth analysis and chronological lifespan (CLS) determination

The *S. cerevisiae* strains used in this paper are reported in Table 1. Yeast cells were grown at 30 °C in minimal medium (Difco Yeast Nitrogen Base without amino acids 6.7 g/L), with 2% w/v glucose and supplements added in excess (Orlandi et al., 2014). Cell growth was monitored by determining cell number using a Coulter Counter-Particle Count and Size Analyser, as described (Vanoni et al., 1983). In parallel, the extracellular concentration of glucose and ethanol were measured in medium samples collected at different time-points using enzymatic assays (K-HKGLU and K-ETOH Megazyme) (Orlandi et al., 2014). Duplication time (Td) was obtained by linear regression of the cell number increase over time on a semi-logarithmic plot. CLS of Fig. 1 was measured according to (Fabrizio et al., 2005) by counting colony-forming units (CFU) starting with 72 h (day 3, first-age point) after diauxic shift (day 0). The number of CFU on day 3 was considered the initial survival (100%). CBSE, dissolved in 20% ethanol by using an ultrasonic bath at 28 khz frequency and 90 W power for 3 min, was added to yeast cultures at the final concentration of 0.2% w/v. A 25X stock solution was prepared to properly dissolve the raw extract and at the same time to limit perturbations in cell culture medium composition after the supplementation. CLS experiments of Figs. 2 and 3 were performed adding CBSE in the exponential phase, as in (Tripodi et al., 2022). Briefly, cells were pre-grown until mid-late exponential phase and then inoculated at 0.150 OD/mL into flasks containing fresh medium in the presence of CBSE at the final concentration of 0.05%, 0.1% or 0.2% w/v. Then, the medium was filtered through 0.22 μm filters and 0.1 mM ampicillin was added to preserve sterility throughout the duration of the experiments. Survival was assessed by propidium iodide staining (PI) at different time points with the Cytoflex cytofluorimeter (Beckman Coulter) and analysed with the Cytoflex software.

2.6. Analysis of reactive oxygen species (ROS) levels

ROS levels were analysed as previously reported (Tripodi et al., 2022). Briefly, yeast cells were collected after 24 h treatment with the extract and 0.2 OD of cells were resuspended in PBS and stained with 5 μg/mL dihydroethidium (DHE) for 10 min. FACS analyses were performed with a Cytoflex cytofluorimeter (Beckman Coulter) and analysed with the Cytoflex software.

2.7. Protein extraction and immunoblotting from yeast proteins

Equal amounts of cells were collected and quenched using TCA 6% and lysed in lysis buffer (6M UREA, 1% SDS, 50 mM Tris-HCl pH7.5, 5 mM EDTA), as reported in (Tripodi et al., 2022). Western blot analysis was performed using anti-GFP antibody (Roche), anti-α-synuclein antibody (Sigma Aldrich) or anti-Cdc34 antibody (Coccetti et al., 2008).

2.8. Analysis of aggresomes in yeast

The intracellular protein aggresomes were analysed using the PROTEOSTAT® Aggresome detection kit (ENZO Life Sciences). Cells were collected following a 24 h treatment with 0.2% CBSE and 0.2 OD were suspended in PBS buffer and stained with the PROTEOSTAT® Aggresome detection reagent at a dilution of 1:1500 (Tripodi et al., 2022). FACS analyses were conducted using a Cytoflex cytofluorimeter (Beckman Coulter) and analysed with Cytoflex software.

2.9. In vitro aggregation of α-syn and ThT assay

α-syn was purchased from Merck and dissolved at 70 μM in PBS. Protein samples (20 μL) were incubated at 37 °C in PBS up to 72 h under constant shaking at 900 rpm with a thermo-mixer in the absence (cnt) or in the presence of the extract at 0.1 and 0.025 mg/mL or in the presence

A

Strain	Td (h)
wt [empty]	2.44 ± 0.38
wt [α-syn]	2.49 ± 0.36

B

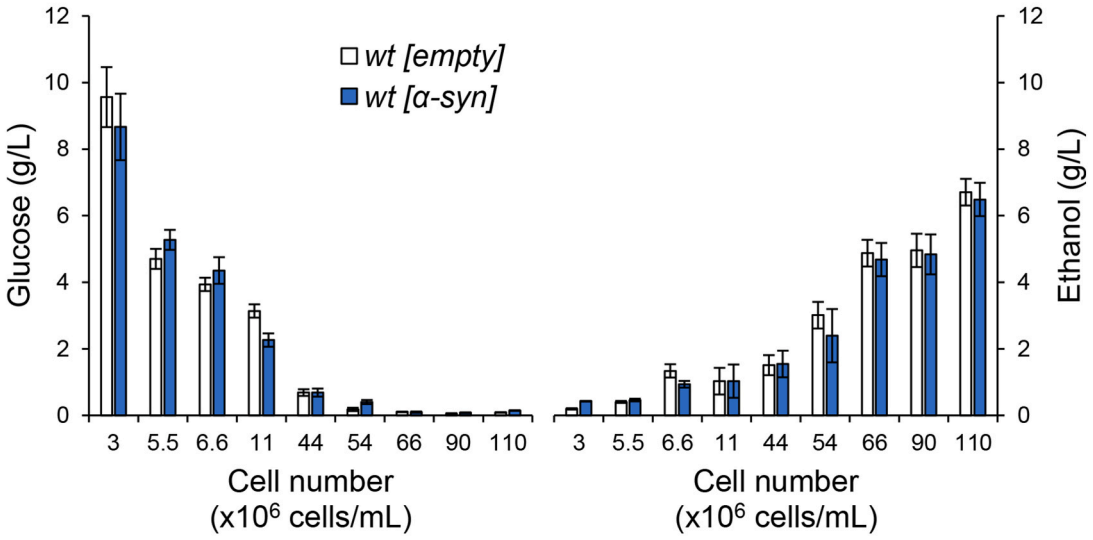

C

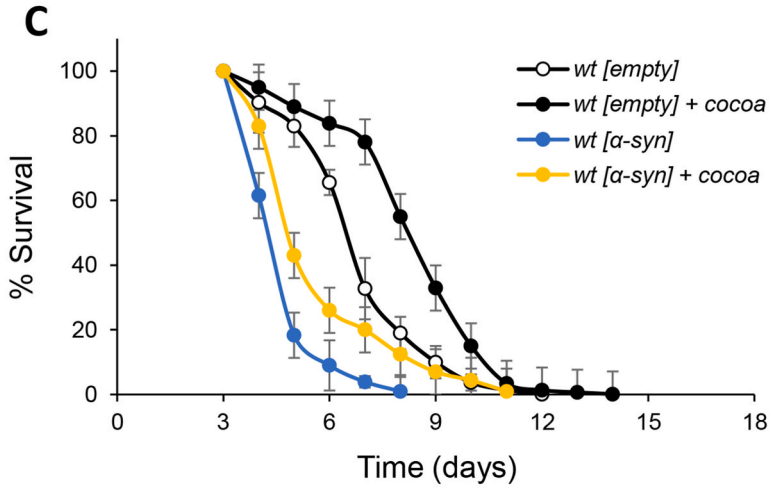

D

Strain	Mean CLS	Max CLS	SI CLS curve
wt [empty]	6.45 ± 0.40	8.93 ± 0.45	315.50 ± 22.01
wt [empty] + cocoa	8.26 ± 0.41**	10.38 ± 0.51**	435.20 ± 21.76**
wt [α-syn]	4.22 ± 0.21**	5.60 ± 0.28**	138.75 ± 6.92**
wt [α-syn] + cocoa	4.79 ± 0.24**	8.22 ± 0.41*	262.50 ± 13.11**

Fig. 1. CBSE supplementation at the diauxic shift extends CLS. Wild-type (*wt[empty]*) and α-syn overexpressing (*wt[α-syn]*) cells were grown in minimal medium containing 2% glucose and required supplements in excess. (A) Cell growth was monitored by counting cell number over time and duplication time (Td) of wt and α-syn expressing cells was calculated as ln2/k, where k is the constant rate of exponential growth. In parallel, (B) extracellular concentration of (left) glucose and (right) ethanol were measured in medium samples collected at different time-points. At the diauxic shift (day 0), CBSE (cocoa) was added and (C) survival over time of the indicated strains was assessed by colony-forming capacity on YEPD plates. 72 h after the diauxic shift (day 3) was considered the first age-point, corresponding to 100% survival. (D) Quantification of chronological survival: data referring to the time-points (days) where chronological aging cultures showed 50% (Mean CLS) and 10% (Max CLS) of survival, as well as, survival integral (SI) measured as reported (Murakami and Kaeberlein, 2009). All data refer to mean values determined in three independent experiments with three technical replicates each. Standard deviations (SD) are indicated. *$p \leq 0.05$ and **$p \leq 0.01$.

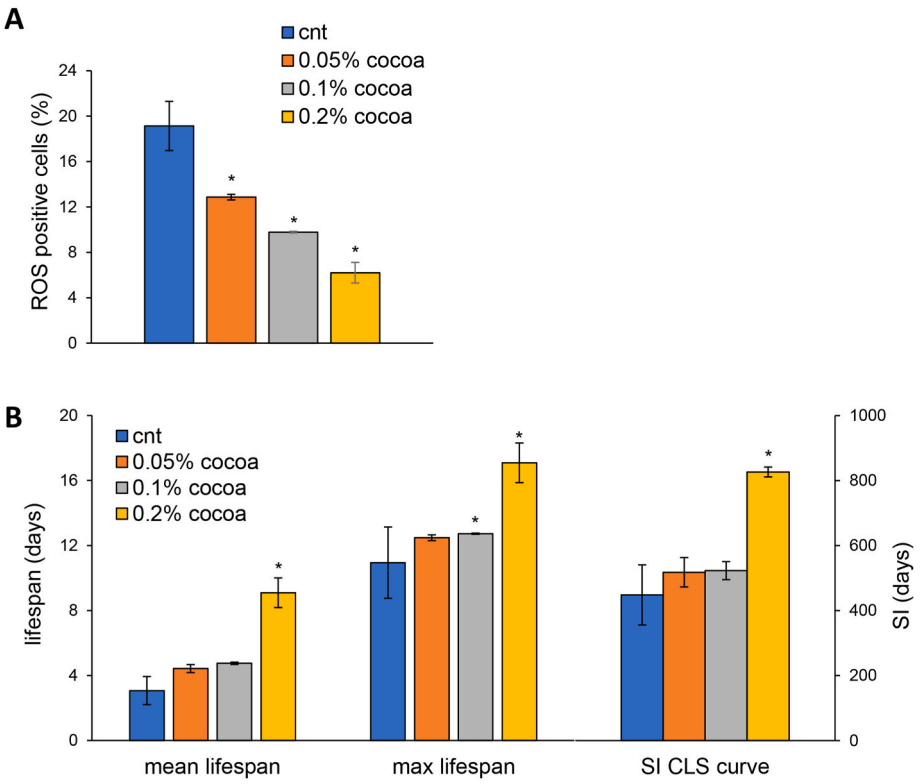

Fig. 2. The CBSE extends yeast lifespan and reduces ROS levels. (A) ROS content of yeast *wt[α-syn]* cells grown in medium containing 2% glucose in the absence or presence of 0.05%, 0.1% or 0.2% CBSE, added in the exponential phase of growth. (B) Mean and maximal lifespan and SI of cells in (A). Histograms represent mean ± standard deviation of at least two independent experiments. *p < 0.05.

of caffeine and theobromine solution at 0.01 mg/mL. The ThT binding assay was performed according to (LeVine, 1999), using a 20 μM ThT solution in PBS buffer. 180 μL of ThT solution were added to 20 μL of the aggregated α-syn samples, transferred into a black 96-well clear bottom multiwell plate and ThT fluorescence was read at the maximum intensity of fluorescence of 485 nm using a Victor X3 plate reader (PerkinElmer); fluorescence of blank samples was subtracted from the fluorescence values of all samples. In control experiments, no interference of the extract on ThT fluorescence was observed.

2.10. Surface plasmon resonance (SPR) analysis

The BIACORE X100 system (Cytiva-Pall) was utilised to analyse molecular interactions between α-syn and the CBSE via Surface Plasmon Resonance (SPR). α-syn was immobilised onto a carboxymethylated dextran surface of a CM5 sensor chip using amine-coupling chemistry, as recommended by the manufacturer (Biacore Sensor Surface handbook BR100571), with the instrument temperature set at 25 °C. The amine coupling procedure was performed using HBS-EP running buffer (0.01 M HEPES, 0.15 M NaCl, 0.003 M EDTA, and 0.005% v/v Surfactant P20, pH 7.4) at a flow rate of 5 μL/min. The CM5 sensor chip was activated by injecting EDC/NHS (1:1) into both flow cells 1 and 2 for 10 min. α-syn was then injected into flow cell 2 at a concentration of 200 μg/mL in 10 mM sodium acetate, pH 3.1, and covalently immobilised at level of 1200 Response Units (RU). The remaining activated sites on the chip were subsequently blocked using 1 M ethanolamine (pH 8.5) in both cells. The association capacity of α-syn was determined by injecting two control antibodies, anti-α-syn (Sigma) recognizing the whole α-syn (positive control) and anti-α-syn33 (Sigma) recognizing α-syn oligomers (negative control), at a dilution of 1:2500 in HBS-EP running buffer at a flow rate of 10 μL/min. The lyophilized CBSE was resuspended in HBS-EP running buffer and injected at multiple concentrations for 5 min at 25 °C and a flow rate of 10 μL/min, with the running buffer injected as a blank under the same conditions. After injection, the analyte solutions were replaced by the running buffer at a continuous flow rate of 10 μL/min for 5 min. Surface regeneration was achieved by injecting 50 mM NaOH for a contact time of 1 min. Each sensorgram was corrected for the response observed in the control flow cell 1 (no immobilised protein) and normalized to a baseline of 0 RU. The sensorgram curves were acquired using the BiacoreX100 Control software, version 2.0.2 (Cytiva-Pall), in manual run mode.

2.11. Biolog OmniLog system

The effect of CBSE was evaluated for its impact on metabolic abilities using various chemical agents. This was done using the Biolog OmniLog Phenotype MicroArray chemical sensitivity panels PM21-PM25, which include 120 chemical compounds at four different concentrations. The Biolog OmniLog System was employed to compare the chemical sensitivity for each drug of *wt[αsyn]* yeast cells with and without 0.2% CBSE. All plates were prepared following the manufacturer's instructions as outlined in the OmniLog ID System User Guide (Biolog). Yeast cell cultures were grown on agar plates at 30 °C and inoculated into 8 mL of minimal medium containing 2% glucose and YNB in sterile glass tubes. The cell suspension was measured using the BIOLOG Turbidimeter (Biolog) until a transmittance of 62% T was achieved. The suspension was prepared according to the BIOLOG PM protocol for yeast cells, using Dye E. 100 μL of cell suspension was added to each well and microplates were incubated in the OmniLog™ system at 30 °C for 72 h. The resistance and sensitivity profiles were compared using the appropriate OmniLog Biolog database (Biolog), with the y-maximum value of each kinetic growth curve being used for the analysis. Ratio between CBSE-treated and control cells were calculated, and compounds which showed a fold change >5 or <0.2 in at least three concentrations for each compound were considered as compounds towards which CBSE increases or decreases sensitivity.

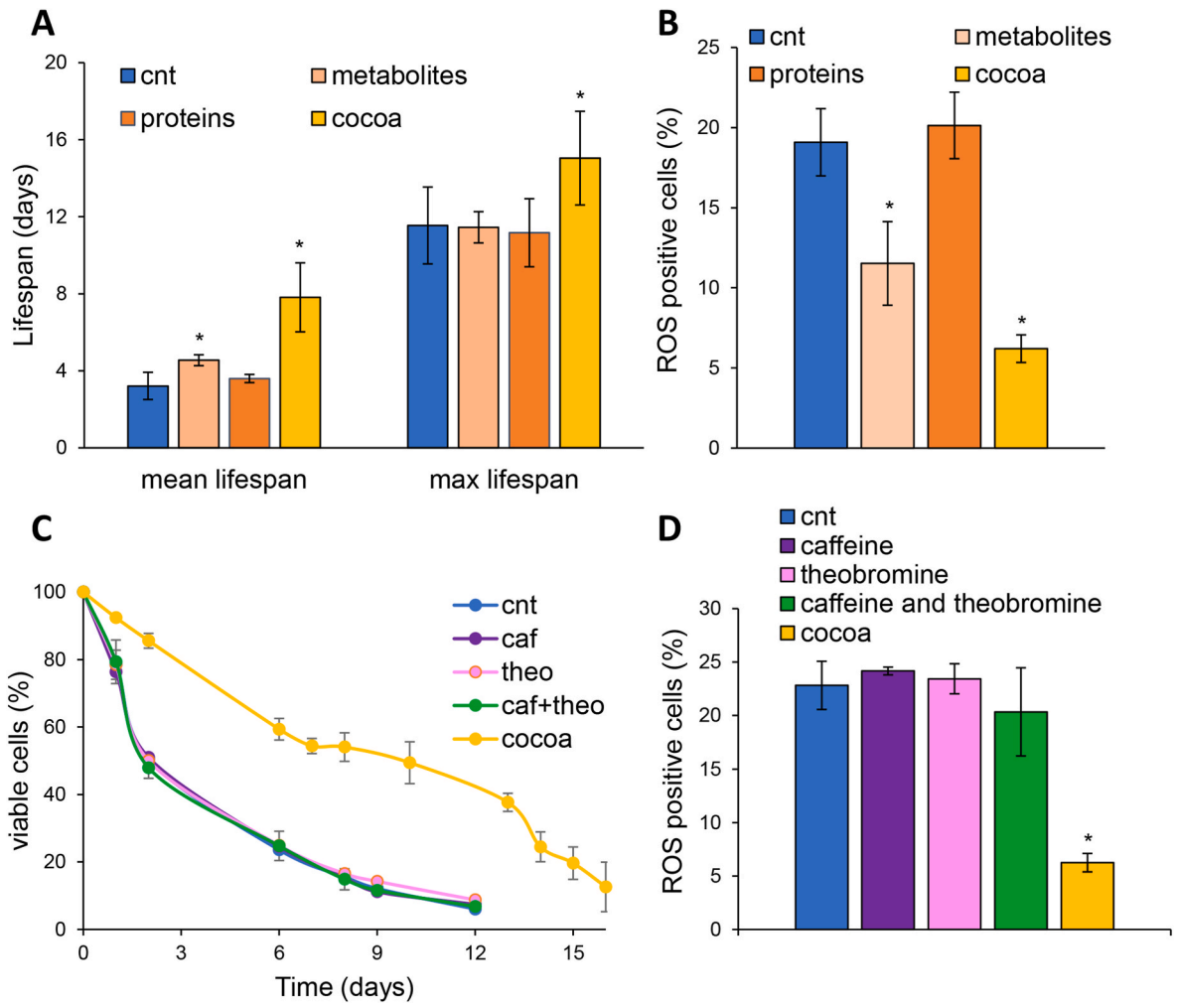

Fig. 3. The effect of the CBSE is independent from caffeine and theobromine. (A) CLS of yeast *wt [α-syn]* cells in medium containing 2% glucose in the absence (cnt) or presence of 0.2% CBSE, and its contained metabolites and proteins. (B) ROS content of cells treated for 24 h as in (A). (C) CLS of yeast *wt [α-syn]* cells in medium containing 2% glucose in the absence or presence of 0.2% CBSE, caffeine, theobromine or a combination of the two (25.96 μg/mL caffeine and 105.4 μg/mL theobromine). (D) ROS content of cells treated for 24 h as in (C). Results are reported as the mean ± standard deviation of three independent experiments. *p < 0.05.

2.12. Cell cultures

SH-SY5Y pTet-SNCA-FLAG were purchased from Merck. Cells were cultured on geltrex-coated plates at 37 °C in DMEM/F12 medium, containing 10% fetal bovine serum, 2 mM glutamine, 100 units/mL penicillin and 100 μg/mL streptomycin, in a humidified 5% CO_2 incubator. Doxycycline-inducible α-syn-expressing cells were selected against the antibiotic puromycin with a dose of 2 μg/mL. Induction of α-syn expression was achieved by adding 6 μg/mL doxycycline (doxy, from a 6 mg/mL stock in DMSO) for 48 h or 72 h. The CBSE was resuspended in water, sterile filtered and added to the medium at a final concentration of 150 μg/mL. For immunofluorescence assays, 160.000 cells were seeded on geltrex-coated glass cover slips in wells of a 24 multiwell plate and treated the day after for 48 h.

2.13. Protein extraction and immunoblotting for mammalian proteins

Total cell extracts were prepared using RIPA buffer (50 mM Tris-HCl, pH 7.5, 150 mM NaCl, 0.5% sodium deoxycholate, 1% NP-40, 0.1% SDS) plus protease inhibitor cocktail (Roche), and phosphatase inhibitor cocktail (Merck). Protein concentration was determined using the Bradford protein assay (Bio-Rad). Western blot analysis was performed using anti-α-syn antibody (Merck), anti-phospho-T172-AMPK antibody (Cell Signaling), anti-AMPKα antibody (Cell signalling), anti-p62/SQSTM1 antibody (Merck), anti-phospho-Ser555-ULK1 antibody (Merck), anti-ULK1 antibody (Calbiochem) and anti-vinculin antibody (Sigma).

2.14. Immunofluorescence assay

After treating cells with doxycycline (Doxy) alone or in combination with CBSE (Doxy + Cocoa) for 48h, cells were washed with PBS, fixed with 4% formaldehyde for 15 min, and permeabilized with PBS-0.2% Triton X-100 for 10 min. Then, cells were washed three times in blocking solution (PBS-1% BSA), blocked at room temperature for 60 min, and then incubated overnight at 4 °C with the primary antibodies dissolved in blocking solution as follows: anti-oligomer A11 Polyclonal Antibody (1:40, Invitrogen), anti α-syn antibody (1:200, Merck). Then, cells were incubated with anti-rabbit secondary antibody (1:200) conjugated with AlexaFluor488, dissolved in a blocking solution, for 1 h at room temperature shield from light. Glasses were mounted with a DAPI containing mounting solution. The PROTEOSTAT R Protein aggregation assay (ENZO Life Sciences) was used to measure α-syn aggregates in cells as described by the manufacturer's instructions. Briefly, after treating cells as mentioned above, cells were washed carefully twice with 1X PBS, then fixed with 4% formaldehyde for 30 min at room temperature and permeabilized with Permeabilizing solution for 30 min on ice. Following PBS washes, the slides were dispensed in Proteostat dye and incubated

for 30 min at room temperature. All treated slides were washed and mounted with a mounting medium with DAPI for nuclear staining and imaged under a Thunder fluorescence microscope (Leica). Image analysis was performed using the ImageJ software (NIH).

2.15. Statistical Analysis

Experiments were conducted in triplicate. Results are presented as mean values ± standard deviations (SD). Statistical data analyses were made using the two-tailed Student's t-test with significance set at $p < 0.05$, or by one-way ANOVA test (*$p \leq 0.05$ and **$p \leq 0.01$).

3. Results

3.1. Characterization of the cocoa bean shell extract

The cocoa bean shell extract (CBSE), which was optimised and partially characterised previously (Pagliari et al., 2022), was subjected to further analyses to better define its composition. For this purpose, both UPLC-PDA-MS and NMR analyses were performed, and the compounds identified or tentatively identified are described in Tables 2 and 3. The identity of some compounds was achieved on the basis of the accurate mass and the associated errors, isotopic distribution, m/z values comparison with those reported in the literature and using literature databases.

NMR analysis identified and quantified mainly amino acids, such as Ala, Leu, Ile, Val, Phe, Asp, Tyr, and intermediates of TCA cycle such as fumarate, succinate, malate and citrate. The last one, together with lactate and glycerol, were the most abundant ones (Table 2, Fig. S1A). MS analysis revealed the presence of the two methylxanthines, caffeine and theobromine (theobromine: 52.74 ± 8.12 μg/mg extract, caffeine: 12.98 ± 3.96 μg/mg extract), and of other less abundant metabolites, like hydroxy-jasmonic acid sulfate, procyanin B, cyanidin-3-O (2″galloyl)-galactoside, as well as of some unknown compounds that could not be clearly identified (Table 3, Fig. S1B).

According to a Bradford quantification, the extract also contained 6 μg/mg of proteins. Although the amount of protein was very low, a proteomic analysis was performed to achieve a characterization. Mass spectrometry analysis of the proteins present in the extract revealed the presence of 5 proteins from *Theobroma cacao* (Table 4), with Vicilins and a 21 kDa seed protein being the most abundant ones according to peptide intensity, as expected from literature (Rawel et al., 2019). However, we cannot exclude the presence of other proteins not identified due to low level of annotation in the database of *T. cacao,* although both UniProt and NCBI databases were used.

Table 2
Metabolites identified by NMR analysis in the ^{1}H spectrum.

Metabolite	^{1}H chemical shift (ppm)	Multiplicity (J [Hz])	Concentration μg/mg ± SD
Leucine	0.96	d [6.2]	3.37 ± 0.09
Isoleucine	1.01	d [7.1]	1.82 ± 0.02
Valine	1.05	d [7.1]	3.22 ± 0.01
2,3-Butanediole	1.15	d [6.4]	1.51 ± 0.10
Lactate	1.33	d [6.9]	31.56 ± 1.12
Alanine	1.48	d [7.2]	4.64 ± 0.09
Acetate	1.92	s	7.43 ± 0.22
GABA	2.30	t [6.1]	2.42 ± 0.06
Succinate	2.41	s	3.74 ± 0.06
Citrate	2.55	d [15.3]	13.02 ± 0.12
Aspartate	2.82	dd [17.4, 3.8]	1.69 ± 0.01
Glycerol	3.66	dd [11.7, 4.3]	15.90 ± 0.56
Mannitol	3.87	dd [11.9, 2.9]	4.76 ± 0.04
Pyroglutamate	4.18	dd [9.1, 5.9]	7.16 ± 0.03
Malate	4.30	dd [10.2, 2.9]	3.53 ± 0.15
Fumarate	6.53	s	0.08 ± 0.01
Tyrosine	6.9	d [8.4]	1.26 ± 0.02
Phenylalanine	7.43	m	4.03 ± 0.05
Formate	8.46	s	0.46 ± 0.01

3.2. Supplementation of CBSE extends CLS of yeast cells expressing human α-syn

Since yeast *S.cerevisiae* has been extensively employed as model system to study the cytotoxic effects of α-syn in PD and other synucleinopathies (Tenreiro et al., 2017), we wished to test in the context of a standard CLS experiment (Fabrizio and Longo, 2007) whether cocoa-shell treatment might have any ameliorating effect on the age-dependent α-syn-mediated cell death (Büttner et al., 2008). To this end a humanised yeast model of PD overexpressing human α-syn was used. As shown in Fig. 1A, no significant differences were observed in the duplication time (Td) between cells expressing α-syn and wt ones grown on minimal medium in 2% glucose (Fig. 1A). Consistently, during the exponential phase, when growth is sustained by a prevalent fermentation-based metabolism, the glucose decrease was accompanied by ethanol accumulation that in both yeast cultures followed the same kinetics (Fig. 1B). Once defined the growth profile, CBSE was added to both cultures at the onset of chronological aging, namely at the diauxic shift, and CLS was determined by CFU scoring. In line with previous reports (Büttner et al., 2008), α-syn expression reduced CLS (Fig. 1C). Interestingly, CBSE supplementation increased both mean and maximum CLS (Fig. 1C and D), as well as the survival integral (SI, Fig. 1D), defined as the area under the CLS curves (Murakami and Kaeberlein, 2009). Indeed, the SI increased by about 38% for wt and 89% for α-syn expressing cells, indicative of a pro-longevity effect of the CBSE. Starting from these results and being specifically interested in α-syn aggregation and its cytotoxic outcome, subsequent analyses were performed only with cells expressing α-syn.

When CBSE was added to exponentially growing cells, up to 0.2%, no effect on the growth rate was observed (data not shown), while a significant dose-dependent reduction of intracellular ROS was detected 1 day after its addition, supporting an antioxidant effect (Fig. 2A). Nevertheless, both the mean and the maximal CLS, as well as the SI increased (more than 70%) only at the highest concentration (0.2%) (Fig. 2B), in accordance with the results reported above.

3.3. The anti-aging effect is independent from caffeine and theobromine

Since the CBSE contains both metabolites and proteins (Tables 2–4), we performed a size-exclusion fractionation to separate the protein fraction (molecular weight >10 kDa) from the metabolite fraction and tested them separately on the yeast model. As shown in Fig. 4A and B, the metabolite fraction increased mean lifespan and reduced ROS levels (albeit to a lesser extent than the total extract), while the protein fraction showed no significant activity, suggesting that metabolites are the main responsible for the antioxidant and anti-aging effect of the CBSE. This is consistent with the very low amount of protein present in the extract.

Among the metabolites identified in the CBSE, caffeine and theobromine represent about 10% of the total extract (see paragraph 3.1). To analyse whether the observed anti-aging effect could be attributed to the presence of these two methylxanthines, α-syn overexpressing cells were treated with caffeine, theobromine or a combination of both, mimicking their abundance in the CBSE. Neither single treatments, nor their combination, showed any anti-aging effect (Fig. 4C) or antioxidant properties (Fig. 4D), suggesting that the pro-longevity function might depend on other metabolites or result from a synergistic/combined action with other molecules of the CBSE.

3.4. The CBSE binds α-syn and reduces its aggregation

In the last years, several data reported that natural extracts could exhibit direct fibrillation-inhibiting effects (Moukham et al., 2024). Thus, we wondered if the anti-aging effect of the CBSE could be due to a

Table 3
Chemical compounds identified or tentatively identified by UPLC-PDA-MS.

m/z expected	m/z calculated	Ionization Mode	Error (ppm)	Molecular formula	Proposed compound	Reference
181.0720	181.0733	M + H	5.5	$C_7H_8N_4O_2$	Theobromine	(Pagliari et al., 2022; Greño et al., 2022)
195.0877	195.0888	M + H	5.9	$C_8H_{10}N_4O_2$	Caffeine	Pagliari et al. (2022)
	263.0636	M + H			Unknown	
	279.0407	M + H			Unknown	
	297.0509	M + H			Unknown	
305.0695	305.0699	M-H	−0.57	$C_{12}H_{18}O_7S$	Hydroxy-jasmonic acid sulfate	Greño et al. (2022)
327.0510	327.0517	M-H	−2.06	$C_{17}H_{12}O_7$	Unknown	
399.0838	399.0835	M + H	0.78	$C_{28}H_{14}OS$	Unknown	
	563.1732	M + H			Unknown	
579.1497	579.1486	M + H	1.90	$C_{30}H_{26}O_{12}$	Procyanidin B	(Pagliari et al., 2022; Alves et al., 2023)
601.1188	601.1183	M + H	0.83	$C_{28}H_{24}O_{15}$	Cyanidin-3-O(2″galloyl)-galactoside	Alves et al. (2023)
	617.0954	M + H			Unknown	
467.1195	467.1214	M-H	−4.07	$C_{21}H_{24}O_{12}$	Unknown	

reduction in α-syn aggregation. A very strong decrease of intracellular aggresomes was observed in yeast cells treated with the CBSE for 24 h, with a 5-fold decrease compared to control cells (Fig. 4A), showing its potential in reducing the aggregation of misfolded proteins. Thus, to evaluate a direct effect of the extract on the aggregation process, α-syn fibrillation experiments were performed *in vitro* and the ThT emission fluorescence signal was used to quantify fibrils formation over time. In the absence of the CBSE, the ThT fluorescence showed the typical sigmoidal shape, indicating the aggregation of the protein; this behaviour completely disappeared in the presence of the extract (at both concentrations, Fig. 4B). Interestingly, caffeine and theobromine together, although had no effect on yeast longevity and ROS content (Fig. 3C and D), showed a partial inhibitory effect on the aggregation of α-syn, Fig. S2A).

A direct effect of the extract on aggregation would imply a direct interaction among the components of the CBSE and α-syn. To explore this hypothesis, α-syn protein was immobilised on a CM5 sensor chip for surface plasmon resonance (SPR) analysis. To validate the suitability and selectivity of the chip, anti α-syn (which binds free and aggregated α-syn) and anti-α-syn33 (which binds only α-syn aggregates) antibodies were utilised as positive and negative controls, respectively, and were injected into the SPR system. While the anti-α-syn antibody bound the protein on the chip, the one specific for the aggregated α-syn showed no binding at all (Fig. S2B). These results showed that the immobilised α-syn protein on the sensor chip surface was in its non-aggregated form and thus was employed to assess its direct binding with the CBSE. Results obtained from the SPR assay indicate that the CBSE could bind to α-syn protein in a concentration-dependent manner (Fig. 4C). Indeed, five increasing concentrations of the extract were tested (0.64 mg/mL, 1.27 mg/mL, 2.54 mg/mL, 5.08 mg/mL and 8 mg/mL) and the response signal increased as a function of the rising concentration of the sample (Fig. 4D). This indicates that there are compounds in the CBSE that directly bind to α-syn, and can explain the inhibitory effect on the amyloid aggregation of α-syn (Fig. 4B). Finally, we tested caffeine and theobromine, which did not appear to bind to the protein (data not shown). However, considering that the molecular weights of caffeine (194.19 g/mol) and theobromine (180.164 g/mol) are near the detection limit of the instrument (100 Da), we cannot exclude that the binding was not detected due to technical limitations.

3.5. The CBSE stimulates autophagy in yeast cells

In an attempt to identify cellular changes occurring upon treatment with the CBSE, a high throughput screening for sensitivity against antibiotics, chemicals and osmolytes was performed. The chemical resistance and sensitivity profile due to the CBSE of the yeast strain overexpressing α-syn was measured using the Biolog Phenotype MicroArrays PM21-PM25 chemical sensitivity panel, which contains 120 assays of chemical sensitivity. Each plate contains 24 different chemical agents in 4 different concentrations, that were divided into 6 groups based on their structure and function: ions, cyclic compounds, organic compounds, chelators, antibiotics, and nitrogen compounds (Table S1). In the presence of 0.2% extract, yeast cells showed increased resistance to several compounds; interestingly most of them have been described for their effect on autophagy in different models (Fig. 5, Table S2).

The autophagic pathway is normally activated in stationary phase cells and is the major process involved in the clearance of α-syn aggregates (Sampaio-Marques et al., 2019). Therefore, to evaluate the activation of the autophagic process in cells treated with the CBSE, we monitored the accumulation of free GFP in cells expressing Atg8-GPF fusion protein, whose cleavage is indicative of autophagy activation. Interestingly, a significant increase in the cleavage of Atg8-GFP was observed 1 day, and even more, 2 days after the extract addition, reflecting the activation of the autophagic process in such condition (Fig.6A,B).

However, in *atg8Δ* cells, CBSE was still able to significantly reduce both intracellular ROS level and aggresomes (Fig. 6C and D), suggesting that the stimulation of the autophagic process is not the only pathway involved in the pro-longevity function of the CBSE.

3.6. The CBSE reduces α-syn aggregates in neuroblastoma cells

In order to further investigate the effects of the CBSE, we turned to SH-SY5Y neuroblastoma cells expressing α-syn under a doxycycline-inducible promoter (Vasquez et al., 2018). As expected, doxycycline induced an increase of monomeric α-syn level, which was not affected by treatment with the CBSE both at 48 h and 72 h (Fig. 7A–C). Although the extract induced the phosphorylation of the energy sensor AMPK, no change of either pULK1 or p62 level was observed, suggesting that the CBSE does not activate the autophagic pathway in neuroblastoma cells (Fig. 7A and B).

One of the key processes for the pathogenesis of Parkinson's disease is the assembly of toxic oligomeric species of α-syn. Then, since we have shown that the CBSE is able to bind and inhibit α-syn aggregation (Fig. 4), the level of α-syn oligomers was investigated in neuroblastoma cells treated with the CBSE. Strikingly, a significant reduction of α-syn oligomers, as well as of intracellular aggresomes were observed upon CBSE treatment (Fig. 7D and E). These data suggest that the CBSE prevents the formation of toxic oligomeric species and not their clearance through the autophagic degradation.

4. Discussion

Accumulation of pathological protein aggregates is associated with a wide range of human diseases. Among these, aggregates of β-amyloid, p-tau or α-syn in the brain are found in patients with Alzheimer's and Parkinson's diseases and correlate with the progression of neurodegeneration (Wilson et al., 2023). Considering the consequent

Table 4
List of proteins by LC-MS^E in cocoa extract with the corresponding peptides.

Entry (Database)	Accession	protein.Description	protein score	MW	protein Matched Products	protein matched Peptides	Cov (%)	Peptide Intensity Sum	Sequence	MH + Error (ppm)	Score
ASP_THECC (Uniprot)	P32765	21 kDa seed protein	615	24438	30	7	30.77	203620	(R)HSDDDGQIR(L)	0.9339	6.6629
									(R)SDLDNGTPVIFSNADSKDDVVR(V)	0.4055	5.9953
									(K)DDVVR(V)	−2.412	5.6277
									(R)VSTDVNIEFVPIR(D)	2.7383	5.3816
									(R)RSDLDNGTPVIFSNADSK(D)	−2.3835	5.2396
									(R)LDNYDNSAGK(W)	−3.3845	5.1266
									(R)ATGQSCPEIVVQR(R)	1.7676	4.8949
A0A061EM85_THECC (Uniprot)	A0A061EM85	Vicilin-A_ putative	200	66198	37	9	17.67	75441	(R)QDRR(E)	−1.8736	6.231
									(K)EQER(G)	−0.3204	5.622
									(K)ELSFGVPSK(L)	1.3752	5.6153
									(R)SEEEEGQQR(N)	−1.5498	5.3042
									(R)GTVVSVPAGSTVYVVSQDNQEK(L)	3.0933	5.2171
									(R)EQEEESEEETFGEFQQVK(A)	1.6377	5.1098
									(R)QQEEELQR(Q)	−3.0807	4.8992
									(R)EKLEEILEEQR(G)	−1.8284	4.7921
									(K)LTIAVLALPVNSPGK(Y)	−0.6553	4.6108
VCL_THECC (Uniprot)	Q43358	Vicilin	167	61483	32	8	17.33	55233	(R)QDRR(E)	−1.8736	6.231
									(K)EQER(G)	−0.3204	5.622
									(R)SEEEEGQQR(N)	−1.5498	5.3042
									(R)GTVVSVPAGSTVYVVSQDNQEK(L)	3.0933	5.2171
									(R)EQEEESEEETFGEFQQVK(A)	1.6377	5.1098
									(R)QQEEELQR(Q)	−3.0807	4.8992
									(R)EKLEEILEEQR(G)	−1.8284	4.7921
									(K)LTIAVLALPVNSPGK(Y)	−0.6553	4.6108
A0A061GTA7_THECC (Uniprot)	A0A061GTA7	Uncharacterized protein	117	10317	4	1	7.53	5242	(K)IEEHQSY(−)	−0.1395	5.2605
A0A061GZ27_THECC (Uniprot)	A0A061GZ27	Putative plant transposon protein domain-containing protein	100	12772	6	1	13.76	6904	(M)NQCHFSEVSCSICQK(V)	0.6846	4.8622
CAA44494.1 (NCBI)	CAA44494.1	vicilin_ partial	1582	54423	81	13	23.7	503177	(R)EQEEESEEETFGEF(−)	0.2798	7.8005
									(R)QDRR(E)	−1.8736	7.1311
									(R)REQEEESEEETFGEF(−)	−0.781	6.6848
									(R)NNPYYFPK(R)	0.4712	6.3261
									(R)DEEGNFK(I)	−1.2679	6.2127
									(R)SEEEEGQQR(N)	−1.5498	6.203
									(K)ESYNVQR(G)	2.3721	6.1794
									(R)GTVVSVPAGSTVYVVSQDNQEK(L)	3.0933	6.1217
									(K)EQER(G)	−1.8439	5.9501
									(R)QQEEELQR(Q)	−3.0807	5.7974
									(R)EKLEEILEEQR(G)	−1.8284	5.6899
									(K)LTIAVLALPVNSPGK(Y)	−0.6553	5.5105
									(K)LEEILEEQR(G)	3.2998	5.3213
									(R)EQEEESEEE(T)	1.8693	0
									(R)EQEEESEEET(F)	1.9878	0
									(R)EQEEESEEETFGE(F)	−1.9716	0
									(R)EQEEESEEETFGEF(−)	0.1171	0
									(R)EQEEESEE(E)	−2.1412	0

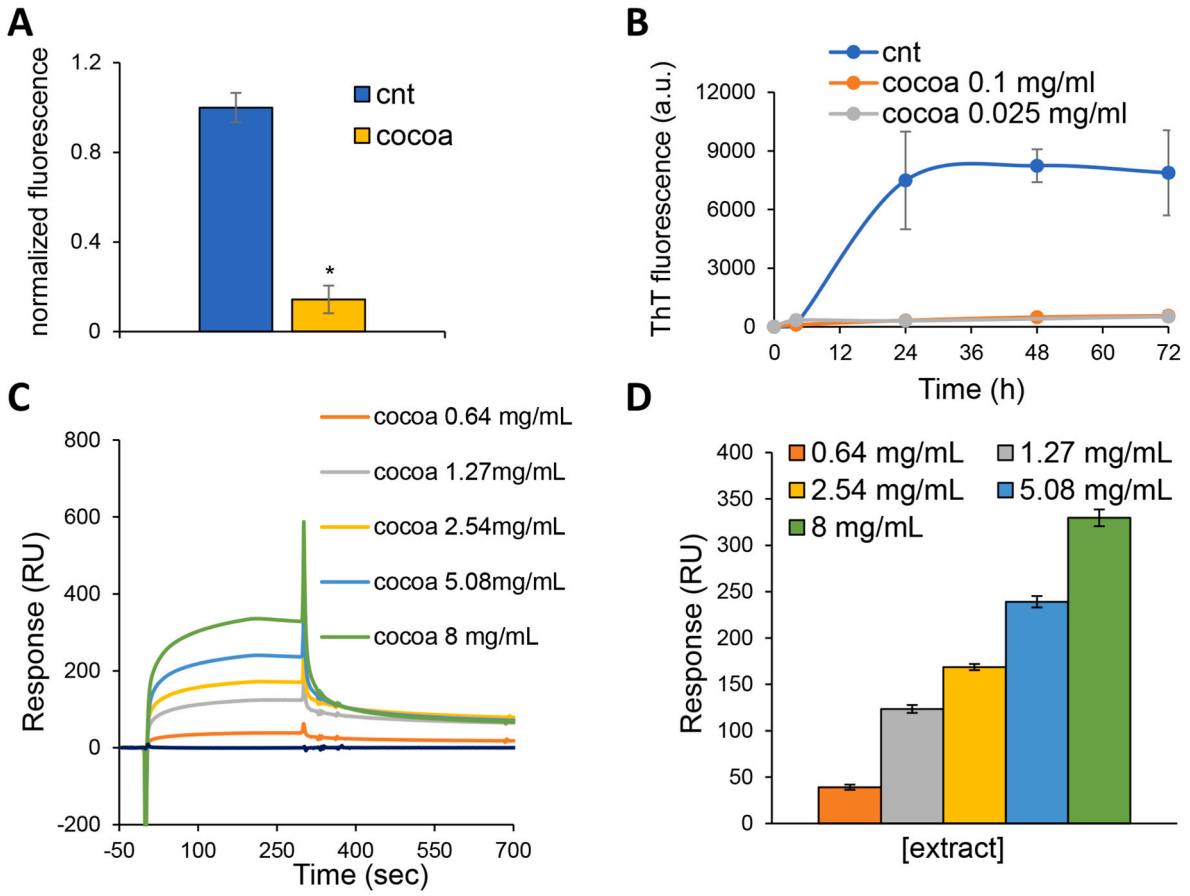

Fig. 4. The CBSE inhibits α-syn aggregation. (A) Fluorescence intensity obtained from flow cytometry analysis of aggresomes of yeast *wt [α-syn]* cells in medium containing 2% glucose in the absence (cnt) or presence of 0.2% CBSE. (B) α-syn aggregation process, followed by ThT fluorescence, in the absence (cnt) or presence of the CBSE (0.1 and 0.025 mg/ml). (C) SPR sensorgrams of CBSE at different concentrations (8 mg/mL, 5.08 mg/mL, 2.54 mg/mL, 1.27 mg/mL, 0.64 mg/mL) display binding toward α-syn on CM5 sensor chip surface. (D) The CBSE shows dose-dependent binding activity to α-syn protein. Results are reported as the mean ± standard deviation of at three independent experiments.

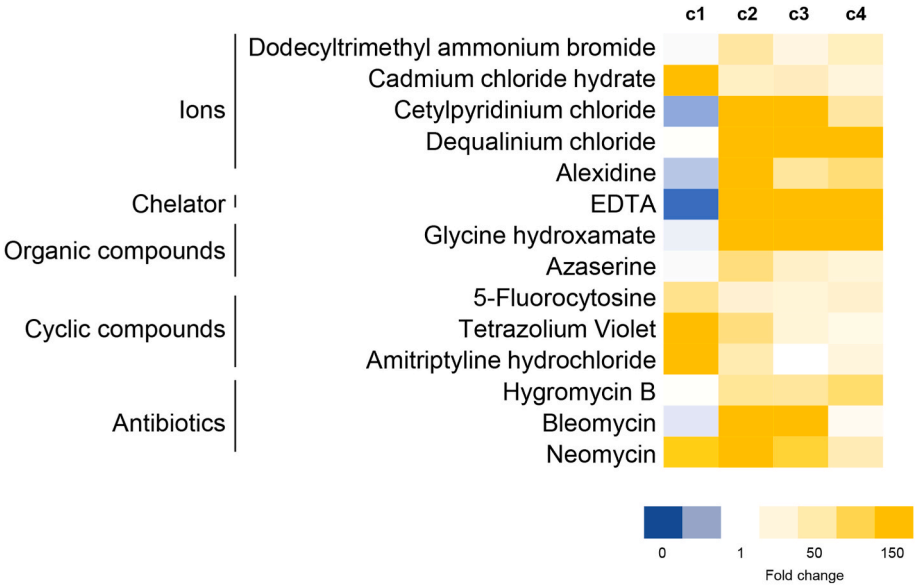

Fig. 5. Drug sensitivity upon CBSE treatment. Heatmap of sensitivity of *wt[α-syn]* cells to selected drugs in the presence of CBSE compared to the control condition, measured by Biolog OmniLog Phenotype MicroArray. Fold changes (treated/cnt) in y-maximum value were calculated and compounds were selected when fold change was >5 or <0.2 in at least three concentrations. Colour scale indicates increased resistance (yellow) or decreased resistance (blue) after 72 h growth.

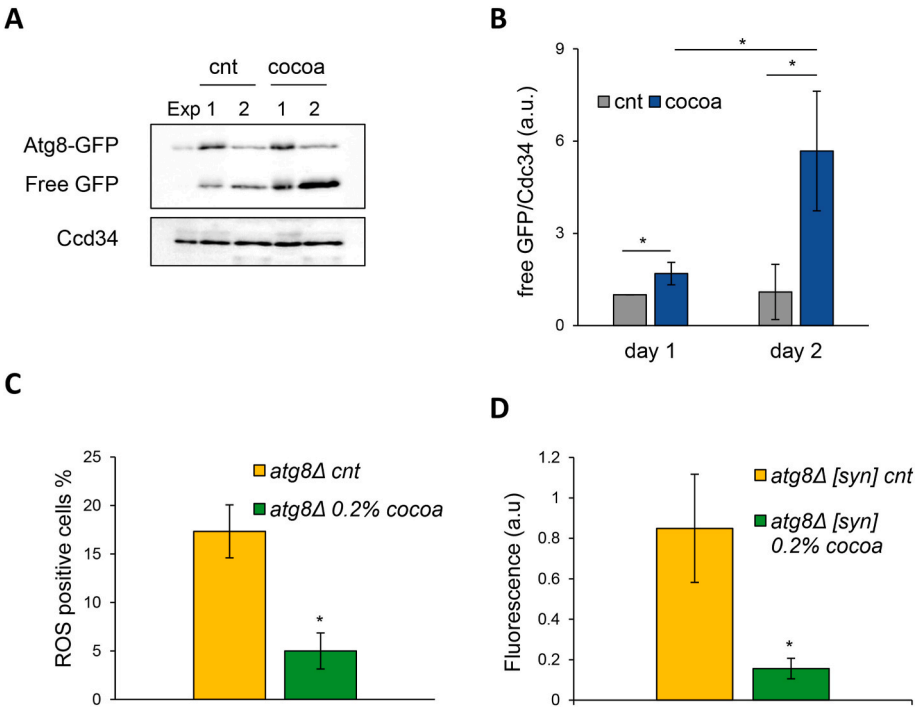

Fig. 6. The CBSE activates autophagy in yeast. (A) Western analysis using anti-GFP antibody on total extracts from *wt[α-syn][Atg8-GFP]* cells treated with 0.2% CBSE for 1 and 2 days. Anti-Cdc34 antibody was used as loading control. (B) Quantification of free GFP of three independent experiments performed as in (A). (C) ROS content of *atg8Δ[α-syn]* cells in medium containing 2% glucose in the absence (cnt) or presence of 0.2% CBSE for 24 h. (D) Fluorescence intensity obtained from flow cytometry analysis of aggresomes of yeast *atg8Δ[α-syn]* cells in medium containing 2% glucose in the absence (cnt) or presence of 0.2% CBSE for 24 h. Results are reported as the mean ± standard deviation. *$p < 0.05$.

induction of neurotoxicity and neuronal loss, there is an increasing interest in the study of secondary metabolites, such as terpenes, flavonoids and phenols, able to inhibit protein aggregation and/or stimulate the clearance of these toxic aggregates. In recent years, the protective effects of a number of bioactive compounds have been highlighted on a wide variety of diseases, among which neurodegenerative ones (Moukham et al., 2024; Pohl et al., 2018).

In the context of the research of still unexplored bioactive molecules, nature is an unlimited reservoir for the discovery of novel therapeutics not only against broad-spectrum diseases, but also for applications in the cosmetic and food industries. In line with this, the valorization of by-products generated by the conventional linear food industry is an emerging strategy to identify new potential useful bioactivities and to reduce food waste.

In the present study we have employed this approach for the utilisation of cocoa bean shells, a by-product typically discarded during the roasting process of cocoa beans (Pagliari et al., 2022).

Here we show that CBSE, obtained by a green extraction and rich in amino acids, organic acids and methylxanthines (Tables 2 and 3), strongly improves yeast longevity and reduces the toxicity of human α-syn, by decreasing intracellular protein aggregates (Figs. 1, 2, 4 and 7). Different eukaryotic models, yeast cells and a neuroblastoma cell line, were used to verify the bioactivity of the CBSE. Although the effects identified are not completely superimposable in the two systems, this approach highlights the importance of using multiple models to better identify all the biological pathways that contribute to the neuroprotective activity of natural compounds. Indeed, while CBSE stimulates autophagy in the yeast model of PD (Fig. 6), this is not the case in neuroblastoma cells, even if the stress responsive kinase AMP-activated protein kinase (AMPK) is activated (Fig. 7). We consider this result particularly relevant because energy metabolism defects are commonly described in neurodegeneration and several studies reported the implication of AMPK in various signalling pathways that are involved in the progression of neurodegeneration (Domise and Vingtdeux, 2016). Thus, the stimulation of both autophagy and AMPK signalling appears to represent as two complementary responses induced by CBSE which together contribute to protect the cell from the toxicity of misfolded proteins.

Results obtained by surface plasmon resonance (SPR) assays indicate also that CBSE binds α-syn protein in a concentration-dependent manner, supporting a direct association of the cacao-bean shell extract with monomers of α-syn by preventing its aggregation into toxic oligomers and amyloid fibrils (Fig. 4B–D). What remains to be elucidated are the specific compounds exerting this role. Although caffeine and theobromine, as well as the very small fraction of proteins contained in the extract, do not have any effect on yeast longevity and ROS content (Fig. 3), the methylxanthines together show a partial inhibitory effect on the aggregation of α-syn *in vitro* (Fig. S2A). The protective functions of methylxanthines are well documented, since they reduce inflammation and preserve cognitive functions (Sánchez et al., 2023; Dong et al., 2020; Eskelinen and Kivipelto, 2010; Valada et al., 2022). Then, the inactivity of both caffeine and theobromine in our yeast model could suggest a possible synergistic or combined role of different molecules within the extract.

The promising results obtained in this study represents the first step for the development of the CBSE as a neuroprotective agent. In order to address if the reported bioactivity may be relevant also under physiological conditions, CBSE bioavailability, absorption rate and metabolism need to be further investigated both in animal models and in clinical studies. In addition, to reach the brain, the active compounds of CBSE have to pass through the gastrointestinal tract and to cross the blood brain barrier, without losing any efficacy. Remarkably, toxicology studies performed in mice, both in acute and sub-chronic assays, indicate that the oral administration of both cacao shell flour or extracts is safe, without significant histopathological alterations (Gil-Ramírez et al., 2024). In line with this, an interesting approach of encapsulation has been reported to enrich chocolate bars with phenolic antioxidant compounds extracted from cocoa bean shells (Grassia et al., 2021).

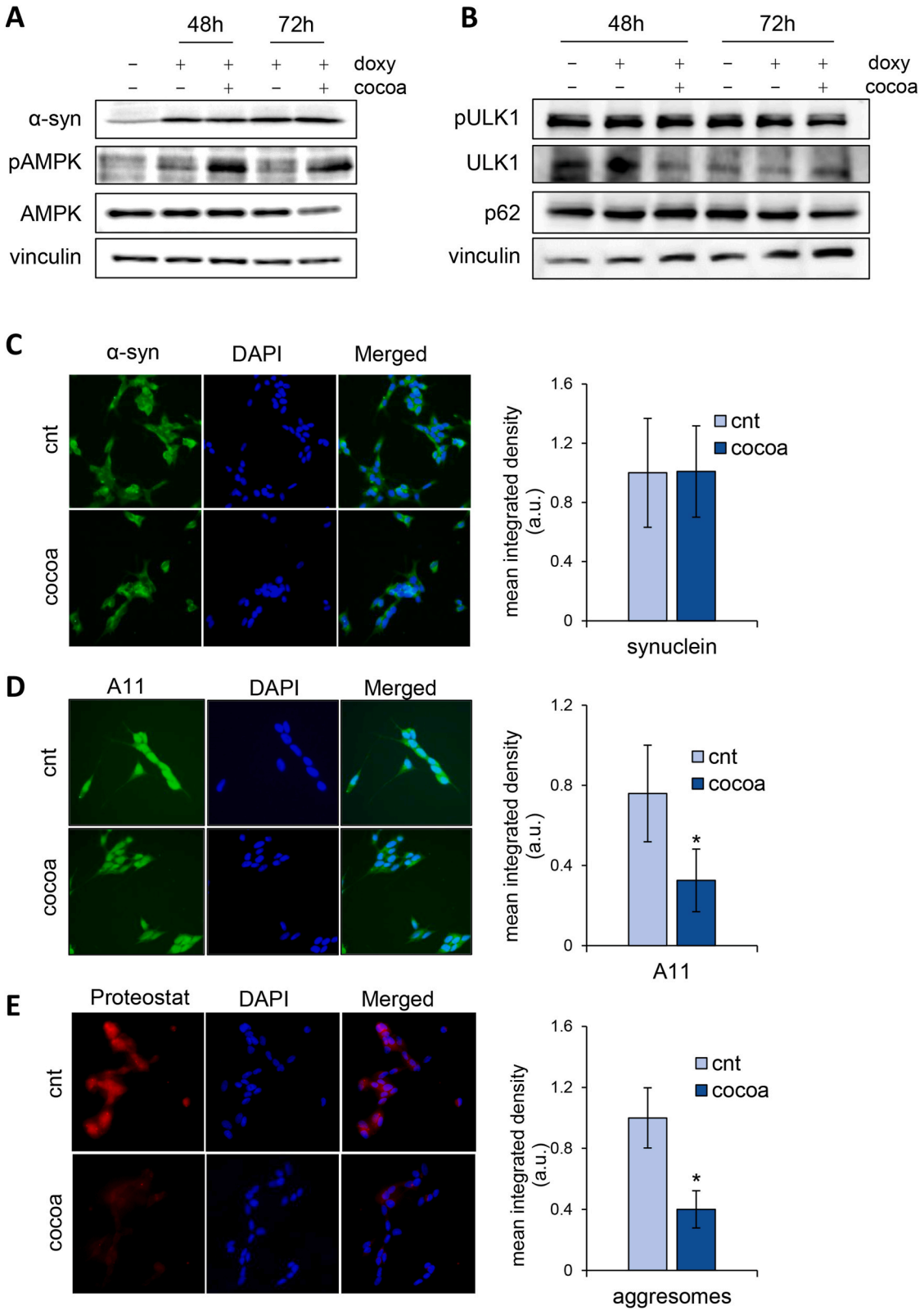

Fig. 7. The CBSE reduces α-syn toxicity in neuroblastoma cells. (A–B) Western blot analysis using anti-α-syn, anti-phospho-T172-AMPK, anti-AMPKα, anti-vinculin antibodies (A) and anti-p62/SQSTM1 anti-phospho-Ser555-ULK1, anti-ULK1 and anti-vinculin antibodies (B) on protein extracts from SH-SY5Y pTet-SNCA-FLAG cells untreated, treated with doxycycline or treated with doxycycline and 150 μg/mL CBSE for 48 and 72 h. (C) Representative immunofluorescence (60x) images of SH-SY5Y cells treated with doxycycline (Doxy) alone and in combination with 150 μg/ml CBSE (Doxy + Cocoa) for 48 h, immunolabeled with anti α-syn antibody (C), A11 anti-oligomer antibody (D), and Proteostat R dye (E). Nuclei were stained by DAPI (Blue). Histograms represent mean ± standard deviation of cell fluorescence quantified with the ImageJ software.

Altogether, our results along with these studies support the potentiality of this waste matrix upcycling as a safe and neuroprotective ingredient for functional foods opening the route to using cocoa bean shell extract, in the form of nutraceutical, as a direct anti-aggregant agent against intracellular protein misfolding and toxicity.

5. Conclusions

During industrial food processing, a large amount of waste is produced. The cocoa bean shell is a valuable by-product of the chocolate industry, thus its valorization may reduce the environmental impact and provide economic benefits. Nowadays, the cocoa bean shells are mainly used for feedstuff, as biofuel and in the agriculture and food industry (Panak Balentić et al., 2018). Here we propose a new valorization approach for this waste product, since through a sustainable, rapid, and cost-effective procedure, we have developed an extract with anti-aggregant properties. Although our study represents the first step towards the use of CBSE as a protective agent, both preclinical and clinical data are still required in the perspective of the development of novel sustainable treatments to prevent neurodegeneration.

CRediT authorship contribution statement

Farida Tripodi: Writing – original draft, Conceptualization, Writing – review & editing. **Alessia Lambiase:** Methodology, Investigation, Formal analysis, Data curation, Visualization. **Hind Moukham:** Methodology, Investigation, Formal analysis, Data curation, Visualization. **Giorgia Spandri:** Methodology, Investigation, Formal analysis, Data curation, Visualization. **Maura Brioschi:** Methodology, Investigation, Formal analysis, Data curation, Visualization. **Ermelinda Falletta:** Methodology, Investigation, Formal analysis, Data curation, Visualization. **Annalisa D'Urzo:** Methodology, Investigation, Formal analysis, Data curation, Visualization. **Marina Vai:** Conceptualization, Writing – review & editing. **Francesco Abbiati:** Methodology, Investigation, Formal analysis, Data curation, Visualization. **Stefania Pagliari:** Methodology, Investigation, Formal analysis, Data curation, Visualization. **Andrea Salvo:** Methodology, Investigation, Formal analysis, Data curation, Visualization. **Mattia Spano:** Methodology, Investigation, Formal analysis, Data curation, Visualization. **Luca Campone:** Methodology, Investigation, Formal analysis, Data curation, Visualization, Funding acquisition, Conceptualization, Writing – review & editing. **Massimo Labra:** Funding acquisition. **Paola Coccetti:** Writing – original draft, Funding acquisition, Conceptualization, Writing – review & editing, Supervision.

Declaration of competing interest

The authors have declared no conflict of interests.

Acknowledgments

This work was supported by the project "ON Foods—Research and innovation network on food and nutrition Sustainability, Safety and Security—Working ON Foods" (CUP:H43C22000820001) of the National Recovery and Resilience Plan (NRRP), Mission 4. Component 2 Investment 1.3—Research funded by the European Union—NextGenerationEU.

This work was also supported by the National Recovery and Resilience Plan (NRRP), Mission 4. Component 2 Investment 1.4—call for tender No. 3138 of December 16, 2021, rectified by Decree No. 3175 of December 18, 2021 of the Italian Ministry of University and Research funded by the European Union—NextGenerationEU; Award Number: Project code CN_00000033, Concession Decree No. 1034 of June 17, 2022. Adopted by the Italian Ministry of University and Research, CUP, H43C22000530001, Spoke 6, Project title "National Biodiversity Future Center—NBFC".

Appendix A. Supplementary data

Supplementary data to this article can be found online at https://doi.org/10.1016/j.crfs.2024.100888.

Data availability

Data will be made available on request.

References

Alves, P.C.C., Guedes, J.A.C., Serrano, L.A.L., et al., 2023. UPLC-QTOF-MS^E-Based metabolic profile to screening candidates of biomarkers of dwarf-cashew clones resistant and susceptible to anthracnose (*Colletotrichum gloeosporioides* (penz) penz. & sacc.). J. Braz. Chem. Soc. 34, 1652–1668. https://doi.org/10.21577/0103-5053.20230097.

Arlorio, M., Coïsson, J.D., Travaglia, F., et al., 2005. Antioxidant and biological activity of phenolic pigments from *Theobroma cacao* hulls extracted with supercritical CO2. Food Res. Int. 38, 1009–1014. https://doi.org/10.1016/j.foodres.2005.03.012.

Avallone, R., Rustichelli, C., Filaferro, M., Vitale, G., 2024. Chemical characterization and beneficial effects of walnut oil on a Drosophila melanogaster model of Parkinson's disease. Molecules 29, 4190. https://doi.org/10.3390/molecules29174190.

Brioschi, M., Lento, S., Tremoli, E., Banfi, C., 2013. Proteomic analysis of endothelial cell secretome: a means of studying the pleiotropic effects of Hmg-CoA reductase inhibitors. J. Proteonomics 78, 346–361. https://doi.org/10.1016/j.jprot.2012.10.003.

Brioschi, M., Eligini, S., Crisci, M., et al., 2014. A mass spectrometry-based workflow for the proteomic analysis of in vitro cultured cell subsets isolated by means of laser capture microdissection. Anal. Bioanal. Chem. 406, 2817–2825. https://doi.org/10.1007/s00216-014-7724-9.

Büttner, S., Bitto, A., Ring, J., et al., 2008. Functional mitochondria are required for alpha-synuclein toxicity in aging yeast. J. Biol. Chem. 283, 7554–7560. https://doi.org/10.1074/jbc.M708477200.

Cadoná, F.C., Dantas, R.F., de Mello, G.H., Silva-Jr, F.P., 2022. Natural products targeting into cancer hallmarks: an update on caffeine, theobromine, and (+)-catechin. Crit. Rev. Food Sci. Nutr. 62, 7222–7241. https://doi.org/10.1080/10408398.2021.1913091.

Calabresi, P., Mechelli, A., Natale, G., et al., 2023. Alpha-synuclein in Parkinson's disease and other synucleinopathies: from overt neurodegeneration back to early synaptic dysfunction. Cell Death Dis. 14, 1–16. https://doi.org/10.1038/s41419-023-05672-9.

Caligiani, A., Acquotti, D., Cirlini, M., Palla, G., 2010. 1H NMR study of fermented cocoa (Theobroma cacao L.) beans. J. Agric. Food Chem. 58, 12105–12111. https://doi.org/10.1021/jf102985w.

Caligiani, A., Palla, L., Acquotti, D., et al., 2014. Application of 1H NMR for the characterisation of cocoa beans of different geographical origins and fermentation levels. Food Chem. 157, 94–99. https://doi.org/10.1016/j.foodchem.2014.01.116.

Cinar, Z.Ö., Atanassova, M., Tumer, T.B., et al., 2021. Cocoa and cocoa bean shells role in human health: an updated review. J. Food Compos. Anal. 103, 104115. https://doi.org/10.1016/j.jfca.2021.104115.

Coccetti, P., Tripodi, F., Tedeschi, G., et al., 2008. The CK2 phosphorylation of catalytic domain of Cdc34 modulates its activity at the G1 to S transition in Saccharomyces cerevisiae. Cell Cycle 7, 1391–1401.

da Silva, L.P.D., da Cruz Guedes, E., Fernandes, I.C.O., et al., 2024. Exploring Caenorhabditis elegans as Parkinson's disease model: neurotoxins and genetic implications. Neurotox. Res. 42, 11. https://doi.org/10.1007/s12640-024-00686-3.

Delenclos, M., Burgess, J.D., Lamprokostopoulou, A., et al., 2019. Cellular models of alpha–synuclein toxicity and aggregation. J. Neurochem. 150, 566. https://doi.org/10.1111/jnc.14806.

Domise, M., Vingtdeux, V., 2016. AMPK in neurodegenerative diseases. Exper. Suppl. (Basel) 107, 153–177. https://doi.org/10.1007/978-3-319-43589-3_7.

Dong, X., Li, S., Sun, J., et al., 2020. Association of coffee, decaffeinated coffee and caffeine intake from coffee with cognitive performance in older adults: national health and nutrition examination survey (NHANES) 2011–2014. Nutrients 12, 840. https://doi.org/10.3390/nu12030840.

Dovonou, A., Bolduc, C., Soto Linan, V., et al., 2023. Animal models of Parkinson's disease: bridging the gap between disease hallmarks and research questions. Transl. Neurodegener. 12, 36. https://doi.org/10.1186/s40035-023-00368-8.

Eskelinen, M.H., Kivipelto, M., 2010. Caffeine as a protective factor in dementia and Alzheimer's disease. J Alzheimers Dis 20 (Suppl. 1), S167–S174. https://doi.org/10.3233/JAD-2010-1404.

Fabrizio, P., Longo, V.D., 2007. The chronological life span of Saccharomyces cerevisiae. Methods Mol. Biol. 371, 89–95. https://doi.org/10.1007/978-1-59745-361-5_8.

Fabrizio, P., Gattazzo, C., Battistella, L., et al., 2005. Sir2 blocks extreme life-span extension. Cell 123, 655–667. https://doi.org/10.1016/j.cell.2005.08.042.

Fields, C.R., Bengoa-Vergniory, N., Wade-Martins, R., 2019. Targeting alpha-synuclein as a therapy for Parkinson's disease. Front. Mol. Neurosci. 12. https://doi.org/10.3389/fnmol.2019.00299.

Fruhmann, G., Seynnaeve, D., Zheng, J., et al., 2017. Yeast buddies helping to unravel the complexity of neurodegenerative disorders. Mechanisms of ageing and development 161, 288–305. https://doi.org/10.1016/J.MAD.2016.05.002.

Gil-Ramírez, A., Cañas, S., Cobeta, I.M., et al., 2024. Uncovering cocoa shell as a safe bioactive food ingredient: nutritional and toxicological breakthroughs. Future Foods 10, 100461. https://doi.org/10.1016/j.fufo.2024.100461.
Grassia, M., Messia, M.C., Marconi, E., et al., 2021. Microencapsulation of phenolic extracts from cocoa shells to enrich chocolate bars. Plant Foods Hum. Nutr. 76, 449–457. https://doi.org/10.1007/s11130-021-00917-4.
Greño, M., Herrero, M., Cifuentes, A., et al., 2022. Assessment of cocoa powder changes during the alkalization process using untargeted metabolomics. Lebensm. Wiss. Technol. 172, 114207. https://doi.org/10.1016/j.lwt.2022.114207.
Hughes, S., van Dop, M., Kolsters, N., et al., 2022. Using a Caenorhabditis elegans Parkinson's disease model to assess disease progression and therapy efficiency. Pharmaceuticals 15, 512. https://doi.org/10.3390/ph15050512.
LeVine, H., 1999. Quantification of beta-sheet amyloid fibril structures with thioflavin T. Methods Enzymol. 309, 274–284. https://doi.org/10.1016/s0076-6879(99)09020-5.
Longo, V.D., Shadel, G.S., Kaeberlein, M., Kennedy, B., 2012. Replicative and chronological aging in saccharomyces cerevisiae. Cell Metabol. 16, 18–31. https://doi.org/10.1016/j.cmet.2012.06.002.
Mazzutti, S., Gonçalves Rodrigues, L.G., Mezzomo, N., Venturi, V., Salvador Ferreira, S. R., 2018. Integrated green-based processes using supercritical CO2 and pressurized ethanol applied to recover antioxidant compouds from cocoa (Theobroma cacao) bean hulls. The Journal of Supercritical Fluids 135, 52–59. https://doi.org/10.1016/j.supflu.2017.12.039.
Moukham, H., Lambiase, A., Barone, G.D., et al., 2024. Exploiting natural niches with neuroprotective properties: a comprehensive review. Nutrients 16, 1298. https://doi.org/10.3390/nu16091298.
Murakami, C., Kaeberlein, M., 2009. Quantifying yeast chronological life span by outgrowth of aged cells. J. Vis. Exp. 1156. https://doi.org/10.3791/1156.
Okiyama, D.C.G., Navarro, S.L.B., Rodrigues, C.E.C., 2017. Cocoa shell and its compounds: applications in the food industry. Trends Food Sci. Technol. 63, 103–112. https://doi.org/10.1016/j.tifs.2017.03.007.
Okiyama, D.C.G., Soares, I.D., Cuevas, M.S., et al., 2018. Pressurized liquid extraction of flavanols and alkaloids from cocoa bean shell using ethanol as solvent. Food Res. Int. 114, 20–29. https://doi.org/10.1016/j.foodres.2018.07.055.
Oreopoulou, V., Russ, W., 2007. Utilization of By-Products and Treatment of Waste in the Food Industry. Springer US.
Orlandi, I., Coppola, D.P., Vai, M., 2014. Rewiring yeast acetate metabolism through MPC1 loss of function leads to mitochondrial damage and decreases chronological lifespan. Microb Cell 1, 393–405. https://doi.org/10.15698/mic2014.12.178.
Outeiro, T.F., Lindquist, S., 2003. Yeast cells provide insight into alpha-synuclein biology and pathobiology. Science (New York, N.Y.) 302, 1772–1775. https://doi.org/10.1126/SCIENCE.1090439.
Pagliari, S., Celano, R., Rastrelli, L., et al., 2022. Extraction of methylxanthines by pressurized hot water extraction from cocoa shell by-product as natural source of functional ingredient. Lebensm. Wiss. Technol. 170, 114115. https://doi.org/10.1016/j.lwt.2022.114115.
Panak Balentić, J., Ačkar, Đ., Jokić, S., et al., 2018. Cocoa shell: a by-product with great potential for wide application. Molecules 23, 1404. https://doi.org/10.3390/molecules23061404.
Poewe, W., Seppi, K., Tanner, C.M., et al., 2017. Parkinson disease. Nat. Rev. Dis. Prim. 3, 1–21. https://doi.org/10.1038/nrdp.2017.13.
Pohl, F., Kong, Thoo, Lin, P., 2018. The potential use of plant natural products and plant extracts with antioxidant properties for the prevention/treatment of neurodegenerative diseases: in vitro. Vivo and Clinical Trials. Molecules 23. https://doi.org/10.3390/molecules23123283.
Popova, B., Kleinknecht, A., Braus, G.H., 2015. Posttranslational modifications and clearing of α-synuclein aggregates in yeast. Biomolecules 5, 617–634. https://doi.org/10.3390/biom5020617.
Rawel, H.M., Huschek, G., Sagu, S.T., Homann, T., 2019. Cocoa bean proteins-characterization, changes and modifications due to ripening and post-harvest processing. Nutrients 11, 428. https://doi.org/10.3390/nu11020428.
Rebollo-Hernanz, M., Zhang, Q., Aguilera, Y., et al., 2019. Cocoa shell aqueous phenolic extract preserves mitochondrial function and insulin sensitivity by attenuating inflammation between macrophages and adipocytes in vitro. Mol. Nutr. Food Res. 63, 1801413. https://doi.org/10.1002/mnfr.201801413.
Rebollo-Hernanz, M., Aguilera, Y., Martin-Cabrejas, M.A., Gonzalez de Mejia, E., 2022. Phytochemicals from the cocoa shell modulate mitochondrial function, lipid and glucose metabolism in hepatocytes via activation of FGF21/ERK, AKT, and mTOR pathways. Antioxidants 11, 136. https://doi.org/10.3390/antiox11010136.
Rojo-Poveda, O., Barbosa-Pereira, L., Zeppa, G., Stévigny, C., 2020. Cocoa bean shell-A by-product with nutritional properties and biofunctional potential. Nutrients 12, 1123. https://doi.org/10.3390/nu12041123.
Sampaio-Marques, B., Pereira, H., Santos, A.R., et al., 2018. Caloric restriction rescues yeast cells from alpha-synuclein toxicity through autophagic control of proteostasis. Aging 10, 3821–3833. https://doi.org/10.18632/aging.101675.
Sampaio-Marques, B., Guedes, A., Vasilevskiy, I., et al., 2019. α-Synuclein toxicity in yeast and human cells is caused by cell cycle re-entry and autophagy degradation of ribonucleotide reductase 1. Aging Cell 18, e12922. https://doi.org/10.1111/acel.12922.
Sánchez, M., Laca, A., Laca, A., Díaz, M., 2023. Cocoa bean shell: a by-product with high potential for nutritional and biotechnological applications. Antioxidants 12, 1028. https://doi.org/10.3390/antiox12051028.
Sanz, F.J., Solana-Manrique, C., Muñoz-Soriano, V., et al., 2017. Identification of potential therapeutic compounds for Parkinson's disease using Drosophila and human cell models. Free Radic. Biol. Med. 108, 683–691. https://doi.org/10.1016/j.freeradbiomed.2017.04.364.
Soares, T.F., Oliveira, M.B.P.P., 2022. Cocoa by-products: characterization of bioactive compounds and beneficial health effects. Molecules 27, 1625. https://doi.org/10.3390/molecules27051625.
Spano, M., Goppa, L., Girometta, C.E., et al., 2024. Dehydrated mycelia (*Cordyceps militaris, Grifola frondosa, Hericium erinaceus* and *Laricifomes officinalis*) as Novel Foods: a comprehensive NMR study. Lebensm. Wiss. Technol. 199, 116123. https://doi.org/10.1016/j.lwt.2024.116123.
Tenreiro, S., Rosado-Ramos, R., Gerhardt, E., et al., 2016. Yeast reveals similar molecular mechanisms underlying alpha- and beta-synuclein toxicity. Hum. Mol. Genet. 25, 275–290. https://doi.org/10.1093/hmg/ddv470.
Tenreiro, S., Franssens, V., Winderickx, J., Outeiro, T.F., 2017. Yeast models of Parkinson's disease-associated molecular pathologies. Curr. Opin. Genet. Dev. 44, 74–83. https://doi.org/10.1016/j.gde.2017.01.013.
Tripodi, F., Lombardi, L., Guzzetti, L., et al., 2020. Protective effect of Vigna unguiculata extract against aging and neurodegeneration. Aging (Albany NY) 12, 19785–19808. https://doi.org/10.18632/aging.104069.
Tripodi, F., Falletta, E., Leri, M., et al., 2022. Anti-aging and neuroprotective properties of grifola frondosa and hericium erinaceus extracts. Nutrients 14, 4368. https://doi.org/10.3390/nu14204368.
Valada, P., Alçada-Morais, S., Cunha, R.A., Lopes, J.P., 2022. Thebromine targets adenosine receptors to control hippocampal neuronal function and damage. Int. J. Mol. Sci. 23, 10510. https://doi.org/10.3390/ijms231810510.
Vanoni, M., Vai, M., Popolo, L., Alberghina, L., 1983. Structural heterogeneity in populations of the budding yeast Saccharomyces cerevisiae. J. Bacteriol. 156, 1282–1291.
Vasquez, V., Mitra, J., Perry, G., et al., 2018. An inducible alpha-synuclein expressing neuronal cell line model for Parkinson's Disease1. J Alzheimers Dis 66, 453–460. https://doi.org/10.3233/JAD-180610.
Visioli, F., Bernardini, E., Poli, A., Paoletti, R., 2012. Chocolate and health: a brief review of the evidence. In: Conti, A., Paoletti, R., Poli, A., Visioli, F. (Eds.), Chocolate and Health. Springer, Milan, Milano, pp. 63–75.
Wilson, D.M., Cookson, M.R., Van Den Bosch, L., et al., 2023. Hallmarks of neurodegenerative diseases. Cell 186, 693–714. https://doi.org/10.1016/j.cell.2022.12.032.